Quality Improvement Study

Medicine®

OPEN

Measurement accuracy of lung nodule volumetry in a phantom study

Effect of axial-volume scan and iterative reconstruction algorithm

Han Na Lee, MD, PhD[a], Jung Im Kim, MD, PhD[a,*], So Youn Shin, MD, PhD[b]

Abstract

An axial-volume scan with adaptive statistical iterative reconstruction-V (ASIR-V) is newly developed. Our goal was to identify the influence of axial-volume scan and ASIR-V on accuracy of automated nodule volumetry.

An "adult" chest phantom containing various nodules was scanned using both helical and axial-volume modes at different dose settings using 256-slice CT. All CT scans were reconstructed using 30% and 50% blending of ASIR-V and filtered back projection. Automated nodule volumetry was performed using commercial software. The image noise, contrast-to-noise ratio (CNR), and signal-to-noise ratio (SNR) were measured.

The axial-volume scan reduced radiation dose by 19.7% compared with helical scan at all radiation dose settings without affecting the accuracy of nodule volumetric measurement ($P = .375$). Image noise, CNR, and SNR were not significantly different between two scan modes (all, $P > .05$).

The use of axial-volume scan with ASIR-V achieved effective radiation dose reduction while preserving the accuracy of nodule volumetry.

Abbreviations: 2D = Two-dimensional, APE = absolute percentage volume error, ASIR = adaptive statistical iterative reconstruction, ASIR-V = adaptive statistical iterative reconstruction-V, CNR = contrast-to-noise ratio, FBP = filtered back projection, GEE = generalized estimating equations, GGN = ground glass nodule, IR = iterative reconstruction, MBIR = model-based iterative reconstruction, ROI = region of interest, SD = standard deviation, SNR = signal-to-noise ratio.

Keywords: axial scan, computed tomography, iterative reconstruction, radiation dosage, thorax, volume measurement

1. Introduction

Accurate measurement of a pulmonary nodule is important both for evaluating treatment response in oncology patients and determining further management for an incidentally detected nodule. Measurement of maximum or 2 maximum orthogonal diameters has been conventionally used as it is easy and quick to obtain. However, 2-dimensional (2D) measurement of pulmonary nodules is limited in its ability to evaluate nodule growth and demonstrates poor inter- and intraobserver agreement.[1,2]

Volumetric measurement of a pulmonary nodule has been reported to be more accurate and reproducible than 2D measurement.[3,4] Furthermore, it provides higher sensitivity for detection of nodule growth than 2D measurement because volumetric measurement considers 3D nodule growth.[5] The recent British Thoracic Society and Fleischner society guidelines highlight the importance of volumetric measurement for assessment of lung nodules.[6,7] Previous research has identified several factors that account for variability of volumetric measurement, including nodule characteristics (size, density, and location), technical parameters (software, slice thickness, radiation dose, and reconstruction algorithm), and observer variability.[2,8–11]

Adaptive statistical iterative reconstruction (ASIR) (GE Healthcare, Waukesha, WI) is a widely used iterative reconstruction (IR) algorithm. A combination of filtered back projection (FBP) and 20% to 40% ASIR is usually used because use of ASIR at high strength has been found to be associated with artificial texture and reduced sharpness.[12,13] Model-based iterative reconstruction (MBIR; Veo; GE Healthcare, Waukesha, WI) offers better image quality than FBP and ASIR as a fully IR, but it cannot be usually used in routine practice because of high computational requirements and long reconstruction times.[14] Most recently, a novel algorithm—adaptive statistical iterative reconstruction-V (ASIR-V) (GE Healthcare, Waukesha, WI)—was introduced. This is a hybrid technique algorithm that considers more advanced system noise statistics, object modeling, and added physics modeling.[15] It has the potential for clinically

Editor: Ali Gholamrezanezhad.

The authors received no specific funding for this work

The authors have no conflicts of interest to disclose.

IRB was waived due to phantom study.

All data generated or analyzed during this study are included in this published article [and its supplementary information files].

[a] Department of Radiology, Kyung Hee University Hospital at Gangdong, College of Medicine, Kyung Hee University, Seoul, Republic of Korea, [b] Department of Radiology, Kyung Hee University Hospital, College of Medicine, Kyung Hee University, Seoul, Republic of Korea.

[*] Correspondence: Jung Im Kim, Department of Radiology, Kyung Hee University Hospital at Gangdong, College of Medicine, Kyung Hee University, 892 Dongnam-Ro. Gangdong-Gu, Seoul 05278, Republic of Korea (e-mail: mine147@gmail.com).

How to cite this article: Lee HN, Kim JI, Shin SY. Measurement accuracy of lung nodule volumetry in a phantom study: Effect of axial-volume scan and iterative reconstruction algorithm. Medicine 2020;99:23(e20543).

Received: 17 October 2019 / Received in final form: 30 April 2020 / Accepted: 4 May 2020

http://dx.doi.org/10.1097/MD.0000000000020543

feasible dose reduction with better image quality than conventional ASIR, as well as a shorter image processing time than that of MBIR. Therefore, ASIR-V can be considered conceptually as "augmented ASIR based on MBIR" or "modified MBIR."[16,17]

Conventionally, axial-volume scan with the step and shoot technique has been introduced in pediatric chest CT or coronary angiography CT that can be scanned using a single rotation with a dose reduction by 18% to 40%.[18–21] However, there are limited clinical studies using axial-volume scan for larger *z*-axis coverage.[22–24] A chest phantom study by Seki et al[25] showed that axial-volume scan was not significantly different from 64-helical scan for nodule identification, besides radiation dose with axial-volume scan was slightly higher than that with helical scan. Although previous study by Doo et al[26] assessed the effect of scan type (axial-volume scan vs helical scan) on nodule volumetry, they did not perform precise pairwise comparisons of volumetric measurement and radiation dose between each scan type.

Therefore, the purpose of this study was to evaluate the influence of axial-volume scan, radiation dose settings, and the novel advanced IR, ASIR-V, on accuracy of pulmonary nodule volumetry.

2. Materials and methods

Ethical approval was not necessary because of a phantom study.

2.1. Phantom

A commercially available anthropomorphic chest phantom, multipurpose chest phantom N1 "Lungman" (Kyoto Kagaku Inc., Japan), was used in this study. The phantom measures 43 × 40 × 48 cm in width, length, and height and consists of simulated vascular structures, mediastinum, spine, ribs, and abdomen block. The phantom is filled with air instead of a structure mimicking lung parenchyma, and is made of polyurethane (soft tissue) and epoxy resin (artificial bone). Spherical simulated pulmonary nodules with different diameters and attenuations (diameter 5, 8, 10, 12 mm; attenuation +100 HU, −630 HU for each diameter), were manually attached to the simulated pulmonary vessels of the phantom using double-sided tape.

2.2. CT acquisition and iterative reconstruction

All CT scans were performed using a 256-row detector CT (Revolution CT, GE Healthcare, Milwaukee, WI). The phantom was scanned using a voltage of 120 kVp, and a tube current-time product of 10, 20, 30, 100 mAs. The phantom was scanned with both helical and axial-volume scan modes at each of the 4 radiation dose settings. The following parameters were the same for helical and axial-volume scans: detector collimation, 256 × 0.625 mm; gantry rotation time, 0.5 seconds, field of view, 350 mm; matrix size, 512 × 512 pixels; and scan length, 31 cm. The pitch factor was 0.992 for helical scan; and beam collimation was 128 × 0.625 mm for helical scan, and 256 × 0.625 mm for axial-volume scan. The axial-volume scan was obtained with 2 gantry rotations using Smart Coverage software which can automatically select the optimal number of rotation according to the given scan length. All raw CT data were reconstructed with a slice thickness of 1.25 mm and an increment of 1.25 mm with standard kernel. Subsequently, 8 CT scans with different scan mode and tube current-time product were reconstructed with FBP, 30% of ASIR-V, and 50% ASIR-V algorithms.

2.3. Nodule volumetry measurement with automatic software

Two radiologists (JIK and HNL with 9 and 4 years' experience in chest radiology) independently performed automated volumetric measurement of simulated nodules on each CT scan. One radiologist (HNL) repeatedly performed automated volumetric measurement at an interval of 6 weeks. The readers were blinded to information about CT parameters, and reference size and attenuation of the nodules. All measurements were performed using a commercially available automated volumetry software package (Lung VCAR, version 13.0, GE Healthcare, Milwaukee, WI). By manually placing the center point on the target nodule, the software automatically performed 3D rendering and quantified the volume by automatic selection of a built-in segmentation algorithm that matches the nodule's density and surrounding structure (Fig. 1). We calculated the absolute percentage volume error (APE) with the following equation: (Vn-Vrf)/Vrf, where Vn is the measured nodule volume and Vrf is the corresponding reference nodule volume.

2.4. Objective image quality assessment

Image noise was assessed by measuring the standard deviation (SD) of a region of interest (ROI) at 3 different locations on a workstation (AW version 3.2; GE Healthcare), by 1 radiologist (HNL). Two ROIs were placed in the 2 simulated lung fields (right anteromedial lung near the mediastinum and left posterolateral lung near the chest wall at the level of carina), and 1 ROI was placed in the air outside the chest phantom (3 cm away from the middle anterior chest wall at the level of the heart) at exactly the same location on each image.[27] The 3 SD values were averaged to calculate image noise of each scan. The area of ROIs was 185.3 mm^2

Contrast-to-noise ratio (CNR) and signal-to-noise ratio (SNR) were calculated using the following equations: CNR = (attenuation of the nodule − attenuation of the background lung field)/SD of the background lung field; and SNR = |attenuation of the nodule|/SD of the nodule. CNR and SNR were calculated in the nodule of −630 HU, 12 mm. The area of ROIs placed on the nodule and the background was 74.2 mm^2. Simulated vessels were carefully avoided as much as possible, when ROIs were placed.

2.5. Statistical analysis

APE was compared between helical and axial-volume scans using the adjusted Wilcoxon signed-rank test to account for clustering effect.[28] A generalized estimating equations (GEE) models with an exchangeable correlation were used to evaluate the association between ASIR-V levels and measured APE both in helical and axial-volume scan, considering clustered imaging data set of 8 nodules.

A GEE model was also used to evaluate influencing factors on APE using different scan modes (helical and axial-volume), radiation dose settings (10, 20, 30 and 100 mAs), reconstruction algorithms (FBP, ASIR-V 30% and ASIR-V 50%), nodule type (solid and ground glass nodules [GGNs]) and nodule size (smaller nodules ≤8 mm; and larger nodules >8 mm). The final GEE model was run with the statistically significant main-effects terms and the interaction terms.

For the objective images of noise, CNR, and SNR, the Wilcoxon signed-rank test was used to compare the effects between helical and axial-volume scans at each reconstruction algorithm (FBP, ASIR-V 30%, and ASIR-V 50%). The Friedman test and the post-hoc Conover test were performed to evaluate differences in image

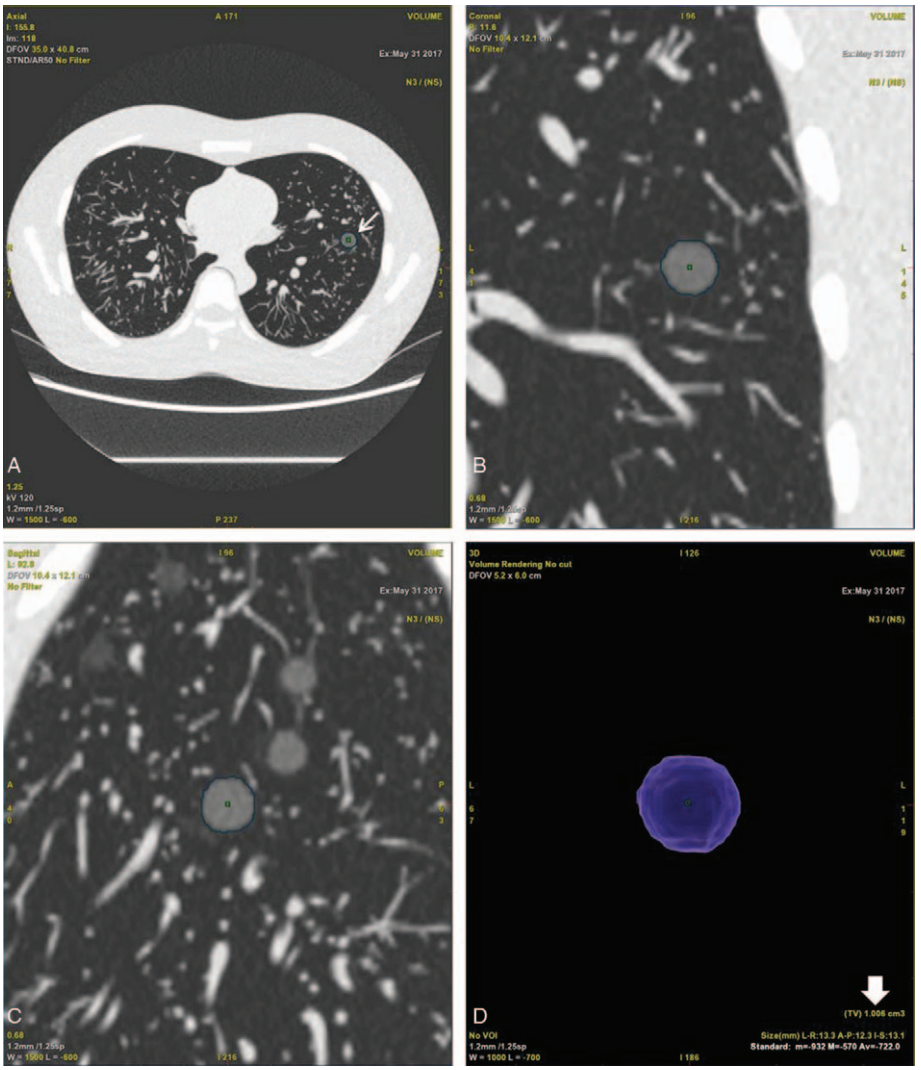

Figure 1. Representative images of volumetric measurement of the nodule (12-mm diameter and −630 HU density) acquired at 120 kVp and 10 mAs using axial-volume scan mode. (A–C) After manual placement of center point on the target nodule (arrows), automatic nodule segmentation is shown on the axial (A), coronal (B), and sagittal (C) images. (D) Three-dimensional volume rendering image shows successfully extracted the nodule volume (arrowhead).

noise, CNR, and SNR among the reconstruction algorithms (FBP, ASIR-V 30%, and ASIR-V 50%).

Bland-Altman analysis was used to evaluate intra- and interobserver agreements within the limit of agreement of mean ± 1.96 SD.[29]

Differences with a P value of <0.05 were considered statistically significant. All statistical analyses were performed with statistical software SPSS version 24.0 (SPSS Inc, Chicago, IL), SAS version 9.4 (SAS Institute Inc., Cary, NC), and MedCalc version 18.2.1 (MedCalc Software, Mariakerke, Belgium).

3. Results

3.1. Helical scan vs. axial-volume scan

The axial-volume scan showed a dose reduction of 19.7% compared to helical scan at all radiation dose settings (Table 1).

Table 1

Radiation dose protocols and dose reduction in axial-volume scan.

		CTDI vol, mGy		DLP, mGy*cm		Effective dose, mSv		
Tube voltage, kVp	Tube current-time product, mAs	Helical	Axial-volume	Helical	Axial-volume	Helical	Axial-volume	Dose reduction (%)
120	10	0.68	0.78	25.28	20.30	0.35	0.28	19.7
	20	1.36	1.56	50.56	40.60	0.71	0.57	19.7
	30	2.04	2.34	75.84	60.90	1.06	0.85	19.7
	100	6.80	7.81	252.80	202.98	3.54	2.84	19.7

CTDI vol = volume dose CT index, DLP = dose-length product.

Conversion factor of 0.014 was used.

Dose reduction of each CT scan was calculated compared to helical scan.

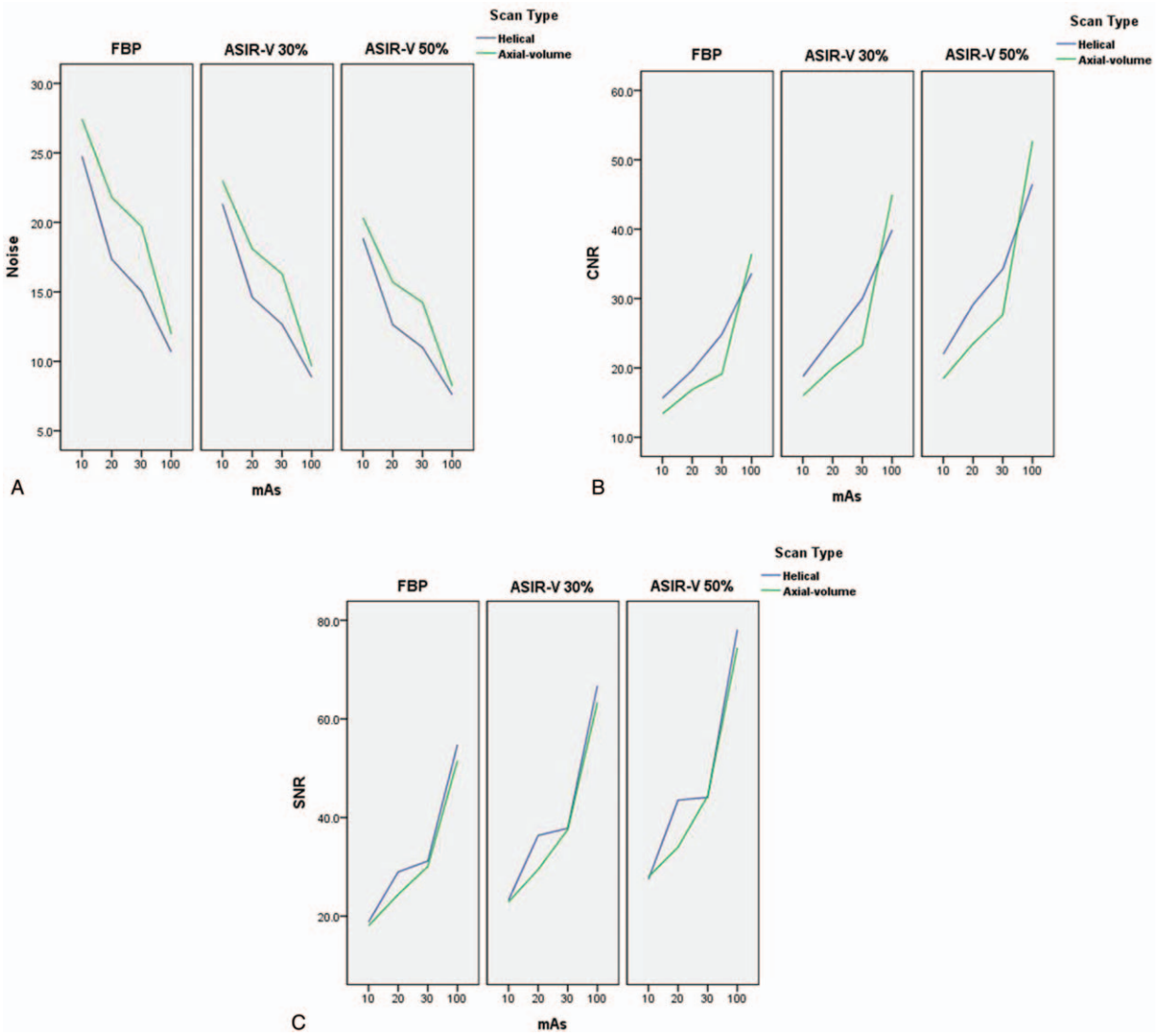

Figure 2. Objective image noise, contrast-to-noise ratio (CNR) and signal-to-noise ratio (SNR) according to different scan modes, iterative reconstructions, and radiation dose settings. (A) In each reconstruction algorithm, image noise was slightly higher in axial-volume scan than in helical scan (right column) ($P > .05$). In both helical and axial-volume scan, noise values were lower in ASIR-V 50% than in other reconstruction algorithms ($P = .018$). (B, C) Significant differences in CNR (B) and SNR (C) were not observed between helical and axial-volume scan ($p > 0.05$). Both CNR and SNR were higher in ASIR-V 50% than in other reconstruction algorithms (all, $P = .018$). FBP = filtered back projection, ASIR-V = adaptive statistical iterative reconstruction V.

There was no significant difference in accuracy of volumetric measurement of nodules between helical and axial-volume scans regardless of the reconstruction algorithms and radiation dose settings used ($P = .375$)

Image noise of the axial-volume scan was slightly higher (16.7%~18.8%) than that of the helical scan with all reconstruction algorithms (FBP: 20.2 ± 6.4 vs 17.0 ± 5.9; ASIR-V 30%: 16.8 ± 5.5 vs 14.4 ± 5.2; and ASIR-V 50%: 14.6 ± 5.0 vs 12.5 ± 4.7) (Fig. 2A). Higher noise level in axial-volume scan was accompanied by a decrease in the mean CNR (FBP: 21.5 ± 20.3 vs 23.4 ± 7.8; ASIR-V 30%: 26.0 ± 13.0 vs 28.3 ± 9.0; and ASIR-V 50%: 30.6 ± 15.2 vs. 33.0 ± 10.3) and the mean SNR (FBP: 31.0 ± 14.5 vs. 33.4 ± 15.2; ASIR-V 30%: 38.3 ± 17.7 vs 14.0 ± 18.3; and ASIR-V 50%: 45.2 ± 20.6 vs 48.3 ± 21.3) compared to that in helical scan (Fig. 2B and 2C). However, the differences in noise, CNR, and SNR between the two scan modes were not statistically significant (all $P > .05$).

3.2. ASIR-V: nodule volumetry and image quality

Figure 3 shows the results of comparison of the APE according to reconstruction algorithms at each radiation dose settings. The mean APEs for FBP, ASIR-V 30%, or ASIR-V 50% were 8.5% ± 5.4%, 8.4% ± 5.9%, and 9.4% ± 6.1%, respectively, in helical scan. In axial-volume scan, the mean APEs for FBP, ASIR-V 30%, or ASIR-V 50% were 7.6% ± 5.5%, 7.4% ± 5.4%, and 6.6% ± 4.7%, respectively. ASIR-V levels did not significantly associat with APE, both in helical ($P = .530$) and axial-volume ($P = .286$) scan (Table 2).

In helical scan, mean image noise was lower by 26.1% (12.53 vs 16.95) for ASIR-V 50% and by 15.2% (14.37 vs 16.95) for ASIR-V 30% compared to FBP. Mean CNR improved by 40.7% (32.97 vs 23.44) for ASIR-V 50%, and 20.5% (28.25 vs 23.44) for ASIR-V 30% versus FBP. Mean SNR improved by 44.5% (48.29 vs 33.43) for ASIR-V 50% and 22.8% (41.04 vs 33.43) for ASIR-V

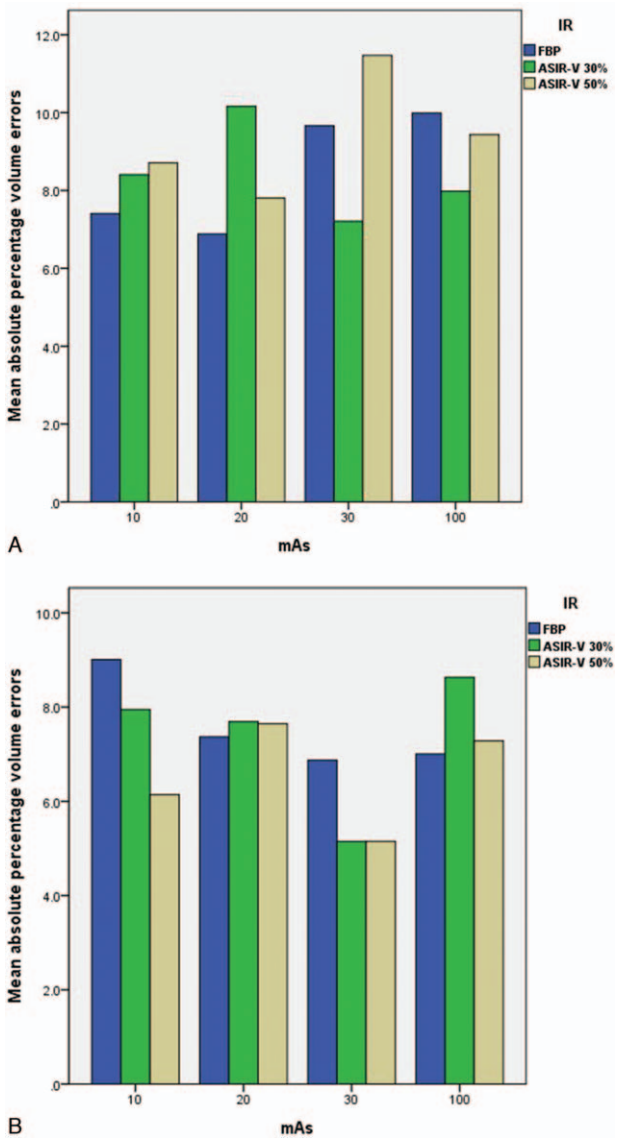

Figure 3. Absolute percentage volume errors (APE) according to reconstruction algorithm. APE were not dependent on reconstruction algorithms (FBP, ASIR-V 30% or ASIR-V 50%), both in helical (A) and axial-volume scan (B). ASIR-V = adaptive statistical iterative reconstruction V, IR = iterative reconstruction, FBP = filtered back projection.

30% versus FBP. Differences in noise, CNR, and SNR among the 3 reconstruction algorithms were statistically significant (all, $P = 0.018$). All pairwise comparisons of noise, CNR, and SNR between reconstruction algorithms demonstrated significant differences in the post-hoc analyses (all, $P < 0.05$) (Fig. 2).

In axial-volume scan, mean noise reduction was 27.7% (14.63 vs 20.23) for ASIR-V 50% and 17.2% (16.76 vs 20.23) for ASIR-V 30% compared with FBP. Mean improvement in CNR was 42.5% (30.57 vs 21.46) for ASIR-V 50%, and 21.4% (26.05 vs 21.46) for ASIR-V 30%. Mean improvement in SNR was 45.7% (45.18 vs 31.01) for ASIR-V 50% and 23.5% (38.29 vs 31.01) for ASIR-V 30% compared with FBP. In axial-volume scan, there were significant differences in noise, CNR, and SNR among the 3 reconstruction algorithms (all, $P = 0.018$). All pairwise comparisons of noise, CNR, and SNR between reconstruction algorithms yielded statistically significant differences in post-hoc analyses (all, $P < 0.05$) (Fig. 2).

3.3. Accuracy of nodule volumetric measurement

In the initial GEE model, radiation dose and reconstruction algorithm were not significantly associated with APE (all, $P > 0.05$); hence, these were excluded from the final GEE model. None of the interaction terms were significant factors (all, $P > 0.05$). The final GEE model demonstrated that GGNs (−630 HU, ß = 4.5, $P < .001$) (simulated GGNs: 10.0% ± 6.5%; simulated solid nodules: 5.9% ± 3.4%), and smaller size (≤8 mm, ß = 4.5, $P < .001$) (smaller nodules: 10.0% ± 6.5%; larger nodules: 5.9% ± 3.4%) were significantly associated with increased APE. Scan mode showed no significant association with APE in the final GEE model ($P = .150$).

3.4. Intra- and interobserver agreement

Interobserver variability in volume measurement ranged from −11.0% to 2.1% (−12.8% to 7.2% for helical scan, and from −14.8% to 2.6% for axial-volume scan). Bland–Altman analysis showed that the intraobserver variability in volume measurement ranged from −7.1% to 5.4% (−15.2% to 4.7% for helical scan and −4.3% to 11.3% for axial-volume scan).

4. Discussion

Our study suggests that automated nodule volumetric measurement is not significantly associated with scan mode, radiation dose setting, or reconstruction algorithm. Axial-volume scan can be applied to low- or ultralow-dose chest CT for volume measurements with preservation of measurement feasibility while considerably reducing radiation dose. A previous study comparing radiation dose between two scan modes in an adult chest phantom has shown that the radiation dose of axial-volume scan with 3 gantry rotations using 320-row detector CT was higher

Table 2

Absolute percentage volume error by different scan mode and reconstruction algorithm.

kVp	mAs	Helical scan						Axial-volume scan					
		FBP		ASIR-V 30%		ASIR-V 50%		FBP		ASIR-V 30%		ASIR-V 50%	
		Mean	95% CI	Mean	95% CI	Mean	95% CI	Mean	95% CI	Mean	95% CI	Mean	95% CI
120	10	7.4 ± 5.8	4.4,12.0	8.4 ± 5.6	5.1,12.9	8.7 ± 5.6	5.3,13.2	9.0 ± 8.4	3.4,15.3	8.0 ± 6.4	4.0,12.3	6.1 ± 4.8	3.1,9.9
	20	6.9 ± 4.3	3.9,10.1	10.2 ± 6.4	6.1,15.2	7.8 ± 4.6	4.5,11.0	7.4 ± 5.1	3.8,11.4	7.7 ± 5.4	3.9,11.8	7.6 ± 5.1	4.3,11.6
	30	9.7 ± 6.3	5.6,14.0	7.2 ± 5.8	3.5,11.5	11.5 ± 8.6	6.2,17.3	6.9 ± 3.9	4.3,9.8	5.1 ± 4.0	2.8,8.1	5.1 ± 4.0	2.8,8.0
	100	10.0 ± 5.5	6.6,13.9	8.0 ± 6.6	3.9,12.7	9.4 ± 5.6	5.4,13.5	7.0 ± 4.4	4.1,10.5	8.6 ± 5.9	4.7,12.6	7.3 ± 5.3	4.0,11.2

All data are indicated as mean value ± standard deviation.

ASIR-V = adaptive statistical iterative reconstruction V, CI = confidence interval, FBP = filtered back projection, GGN = ground glass nodule.

than that of a 64-row detector helical scan.[25] Recently, in a study using 256-row detector CT, Lambert et al reported that the axial-volume scan at short scan lengths was slightly more dose-efficient because the helical overrange represents the predominant additional dose factor; however, the opposite was true at longer scan length because the additional dose contribution from the axial overlaps of axial-volume scan becomes predominant.[30] Vendor difference and the number of axial overlaps according to scan lengths can explain the variation in dose reduction of axial-volume scan reported in previous studies. In this study, axial-volume scan using 256-row detector CT with 2 axial sections achieved a dose reduction of 19.7% compared to helical scan without affecting the accuracy of nodule volumetry.

The increase in the number of axial sections according to longer *z*-axis coverage could not result in significant scan time delay and motion artifacts; however, it results in dislocation and heterogeneity between different axial sections.[22,31] The CT scan parameters such as fast rotation times (~0.28 seconds), rapid table speeds (~300 mm/s), and new software algorithm to correct the dislocation between the edge of axial-volume scan may aid in reducing motion artifact and heterogeneity.[22,24,30]

A small number of recent investigations, mainly phantom-based, have demonstrated that volumetry derived from IR is at least as accurate as FBP with <10% differences in volumetry regardless of IR strength.[2] Also in this study, we identified small differences in mean APE between FBP and ASIR-V 30% or ASIR-V 50% in both helical and axial-volume scans. Although IR strength showed no influence on the accuracy of volumetric measurement, objective image quality was significantly improved with increasing degrees of ASIR-V levels. In this study, image noise with ASIR-V 50% was 12.9% lower than that with ASIR-V 30% regardless of scan mode. Furthermore, a recent study reported that the subjective image noise was significantly lower (10%–15%) for ASIR-V than for ASIR.[32] We could not compare ASIR and ASIR-V because our CT vendor can handle only the ASIR-V reconstruction algorithm.

Low contrast between GGNs and lung parenchyma as well as uneven margin of GGNs leads to poorer volumetric measurement compared to that in solid nodules.[2,33] In previous volumetry phantom studies, mean volumetric measurement errors of GGN ranged from 5% to 15%.[26,34–36] The mean APE, ranging from 7% to 11%, for GGNs (−630 HU) in our study was consistent with results of previous studies and nodule density was significantly associated with volumetric measurement errors. Nodule size is another known crucial factor determining the accuracy and reproducibility of lung nodule volumetry.[33] In a study on nodule volumetry in screening CT, Liang et al[11] reported a marked decrease in measurement variability for nodules >10 mm in diameter. Likewise, in our study, nodule size was imporntant factor determining accuracy of nodule volumetry, when the size of nodule was divided into 2 categories based on diameter of 8 mm.

Our study has several limitations. First, volumetry was conducted on artificial nodules implanted in a chest phantom. Hence, the variability in nodule number and characteristics such as shape, size, margin, and attenuation of nodules encountered in real patients could not be replicated and this is an unavoidable limitation of phantom study. However, we could focus on the effect of nodule size and nodule attenuation because the other nodule features were controlled. Second, we used single commercial automated volumetry software. Substantial variations in segmentation performance between different software packages have been reported.[2] Hence, our results may not be reproducible using different volumetry software.

In conclusion, axial-volume scan for adult chest CT showed a radiation dose reduction of 19.7% compared to helical scan, while preserving the accuracy of nodule volumetry, regardless of the radiation dose settings and iterative reconstruction algorithm used. New iterative reconstruction of ASIR-V provided significant image quality improvement without affecting volume measurement, compared with FBP.

Author contributions

Conceptualization: Jung Im Kim.
Data curation: Han Na Lee, Jung Im Kim.
Investigation: Han Na Lee, Jung Im Kim.
Methodology: Han Na Lee, Jung Im Kim, So Youn Shin.
Supervision: Jung Im Kim.
Validation: So Youn Shin.
Visualization: So Youn Shin.
Writing – original draft: Han Na Lee.

References

[1] Revel MP, Bissery A, Bienvenu M, et al. Are two-dimensional CT measurements of small noncalcified pulmonary nodules reliable? Radiology 2004;231:453–8.
[2] Devaraj A, van Ginneken B, Nair A, et al. Use of volumetry for lung nodule management: theory and practice. Radiology 2017;284:630–44.
[3] Jennings SG, Winer-Muram HT, Tarver RD, et al. Lung tumor growth: assessment with CT–comparison of diameter and cross-sectional area with volume measurements. Radiology 2004;231:866–71.
[4] Marten K, Auer F, Schmidt S, et al. Inadequacy of manual measurements compared to automated ct volumetry in assessment of treatment response of pulmonary metastases using recist criteria. Eur Radiol 2006;16: 781–90.
[5] Ko JP, Berman EJ, Kaur M, et al. Pulmonary nodules: growth rate assessment in patients by using serial ct and three-dimensional volumetry. Radiology 2012;262:662–71.
[6] Bankier AA, MacMahon H, Goo JM, et al. Recommendations for measuring pulmonary nodules at CT: a statement from the fleischner society. Radiology 2017;285:584–600.
[7] Callister MEJ, Baldwin DR, Akram AR, et al. British thoracic society guidelines for the investigation and management of pulmonary nodules: accredited by nice. Thorax 2015;70:ii1–54.
[8] Ashraf H, de Hoop B, Shaker SB, et al. Lung nodule volumetry: segmentation algorithms within the same software package cannot be used interchangeably. Eur Radiol 2010;20:1878–85.
[9] Gietema HA, Schaefer-Prokop CM, Mali WP, et al. Pul-monary nodules: interscan variability of semiautomated volume measurements with multisection CT—influence of inspiration level, nodule size, and segmentation performance. Radiology 2007;245:888–94.
[10] Petrou M, Quint LE, Nan B, et al. Pulmonary nodule volumetric measure-ment variability as a function of CT slice thickness and nodule morphology. AJR Am J Roentgenol 2007;188:306–12.
[11] Liang M, Yip R, Tang W, et al. Variation in screening CT-detected nodule volumetry as a function of size. AJR Am J Roentgenol 2017;209:304–8.
[12] Singh S, Kalra MK, Hsieh J, et al. Abdominal CT: comparison of adaptive statistical iterative and filtered back projection rec-onstruction techniques. Radiology 2010;257:373–83.
[13] Singh S, Kalra MK, Gilman MD, et al. Adaptive statistical iterative reconstruction technique for radiation dose reduction in chest CT: a pilot study. Radiology 2011;259:565–73.
[14] Willemink MJ, de Jong PA, Leiner T, et al. Iterative reconstruction techniques for computed tomography part 1: technical principles. Eur Radiol 2013;23:1623–31.
[15] Benz DC, Grani C, Mikulicic F, et al. Adap-tive statistical iterative reconstruction-V: impact on image quality in ultralow d-ose coronary computed tomography angiography. J Comput Assist Tomogr 2016; 40:958–63.

[16] Lee S, Kwon H, Cho J. The detection of focal liver lesions using abdominal CT: a comparison of image quality between adaptive statistical iterative reconst-ruction vV and adaptive statistical iterative reconstruction. Acad Radiol 2016;23:1532–8.
[17] Kwon H, Cho J, Oh J, et al. The adaptive statistical it-erative reconstruction-V technique for radiation dose reduction in abdominal CT: comparison with the adaptive statistical iterative reconstruction technique. Br J Radiol 2015;88:20150463.
[18] Kroft LJ, Roelofs JJ, Geleijns J. Scan time and patient dose for thoracic imagi-ng in neonates and small children using axial volumetric 320-detector row CT compared to helical 64-, 32-, and 16- detector row CT acquisitions. Pediatr Radiol 2010;40:294–300.
[19] Khan A, Khosa F, Nasir K, et al. Comparison of radiation dose and image quality: 320-MDCT versus 64-MDCT coronary angiography. AJR Am J Roentgenol 2011;197:163–8.
[20] Einstein AJ, Elliston CD, Arai AE, et al. Radiation dose from single-heartbeat coronary CT angiography performed with a 320-detector row volume scanner. Radiology 2010;254:698–706.
[21] Ryu YJ, Kim WS, Choi YH, et al. Pediatric che-st CT: wide-volume and helical scan modes in 320-MDCT. AJR Am J Roentgenol 2015; 205:1315–21.
[22] Honda O, Takenaka D, Matsuki M, et al. Image quality of 320-detector row wide-volume computed tomography with diffuse lung diseases: comparison with 64-detector row helical CT. J Comput Assist Tomogr 2012;36:505–11.
[23] Kitajima K, Maeda T, Ohno Y, et al. Capability of abdominal 320-detector row CT for small vasculature assessment compared with that of 64-detector row CT. Eur J Radiol 2011;80:219–23.
[24] Shah R, Khoram R, Lambert JW, et al. Effect of gantry rotation speed and scan mode on peristalsis motion artifact frequency and severity at abdominal CT. Abdom Radiol (NY) 2018;43:2239–45.
[25] Seki S, Koyama H, Ohno Y, et al. Adaptive iterative dose reduction 3D (AIDR 3D) vs. filtered back projection: radiation dose reduction capabilities of wide volume and helical scanning techniques on area-detector CT in a chest phantom study. Acta Radiol 2016;57:684–90.
[26] Doo KW, Kang EY, Yong HS, et al. Accuracy of lung nodule volumetry in low-dose CT with iterative reconstruction: an anthropomorphic thoracic phantom study. Br J Radiol 2014;87: 20130644.
[27] Kim H, Park CM, Song YS, et al. Influence of radiation dose and iterative reconstruction algorithms for measurement accuracy and reproducibility of pulmonary nodule volumetry: a phantom study. Eur J Radiol 2014;83:848–57.
[28] Kang S-H, Kim HW, Ahn CW. A permutation test for nonindependent matched pair data. Drug Inf J 2001;35:407–11.
[29] Bland JM, Altman DG. Comparing methods of measurement: why plotting difference against standard method is misleading. Lancet 1995;346:1085–7.
[30] Lambert JW, Phillips ED, Villanueva-Meyer JE, et al. Axial or helical? Considerations for wide collimation ct scanners capable of volumetric imaging in both modes. Med Phys 2017;44:5718–25.
[31] Kalisz K, Buethe J, Saboo SS, et al. Artifacts at cardiac CT: physics and solutions. RadioGraphics 2016;36:2064–83.
[32] Lim K, Kwon H, Cho J, et al. Initial phantom study comparing image quality in computed tomography using adaptive statistical iterative reconstruction and new adaptive statistical iterative reconstruction V. J Comput Assist Tomogr 2015;39:443–8.
[33] Goo JM. A computer-aided diagnosis for evaluating lung nodules on chest CT: the current status and perspective. Korean J Radiol 2011;12:145–55.
[34] Oda S, Awai K, Murao K, et al. Computer-aided volumetry of pulmonary nodules exhibiting ground-glass opacity at MDCT. AJR Am J Roentgenol 2010;194:398–406.
[35] Scholten ET, Jacobs C, van Ginneken B, et al. Computer-aided segmentation and volumetry of artificial ground-glass nodules at chest CT. AJR Am J Roentgenol 2013;201:295–300.
[36] Linning E, Daqing M. Volumetric measurement pulmonary ground-glass opacity nodules with multi-detector CT: Effect of various tube current on measurement accuracy—a chest CT phantom study. Acad Radiol 2009;16:934–9.